EWS-CREB1: A Recurrent Variant Fusion in Clear Cell Sarcoma—Association with Gastrointestinal Location and Absence of Melanocytic Differentiation

Cristina R. Antonescu,[1] Khedoudja Nafa,[1] Neil H. Segal,[2] Paola Dal Cin,[3] and Marc Ladanyi[1]

Abstract

Purpose: Clear cell sarcoma (CCS) usually arises in the lower extremities of young adults and is typically associated with a t(12;22) translocation resulting in the fusion of *EWS* (*EWSR1*) with *ATF1*, a gene encoding a member of the cyclic AMP – responsive element binding protein (CREB) family of transcription factors. CCS arising in the gastrointestinal tract is rare and its pathologic and molecular features are not well defined.

Experimental Design: We report a novel variant fusion of *EWS* to *CREB1*, a gene at 2q32 encoding another CREB family member highly related to ATF1, detected in three women with gastrointestinal CCS. All three cases contained an identical *EWS-CREB1* fusion transcript that was shown by reverse transcription-PCR. In two of the cases tested, *EWS* gene rearrangement was also confirmed by fluorescence *in situ* hybridization and the *EWS-CREB1* genomic junction fragments were isolated by long-range DNA PCR.

Results: Morphologically, all three tumors lacked melanin pigmentation. By immunohistochemistry, there was a strong and diffuse S100 protein reactivity, whereas all melanocytic markers were negative. Ultrastructurally, two of the cases lacked melanosomes. The melanocyte-specific transcript of *MITF* was absent in two cases, and only weakly expressed in the third case. The Affymetrix gene expression data available in one case showed lower expression of the melanocytic genes *MITF, TYR*, and *TYRP1*, compared with four *EWS-ATF1*-positive CCSs of non-gastrointestinal origin.

Conclusions: *EWS-CREB1* may define a novel subset of CCS that occurs preferentially in the gastrointestinal tract and shows little or no melanocytic differentiation. Thus, evidence of melanocytic lineage or differentiation is not a necessary feature of sarcomas with gene fusions involving *CREB* family members.

Clear cell sarcoma (CCS), also known as melanoma of soft parts, typically presents in the deep soft tissues of the lower extremity, in close proximity to tendons, fascia, or aponeuroses. Young adults are preferentially affected and the clinical course is often marked by regional and distant metastases. Most CCS show immunoreactivity for melanoma markers, such as HMB45, and contain melanosomes. Indeed, most CCS share a melanocytic gene expression signature with melanomas (1). However, CCS are also genetically distinct from melanomas, as they lack *BRAF* mutations (2) and show, in most cases, a recurrent chromosomal translocation t(12;22)(q13;q12), resulting in the fusion of the *EWS* gene (also known as *EWSR1*) on 22q12 with the *activating transcription factor-1* gene (*ATF1*) on 12q13 (3–6).

Primary CCSs of the gastrointestinal tract are rare (7, 8). Gastrointestinal CCS includes a histologic variant rich in osteoclast-type giant cells which uniformly express S100 protein, but lack melanocytic differentiation by immunohistochemistry, being negative for HMB45 and Mart-1 (9). As a result of its rarity in the gastrointestinal tract, the differential diagnosis of CCS in this site includes more common mesenchymal or neuroectodermal neoplasms, such as gastrointestinal stromal tumors, schwannoma, carcinoid, or metastatic melanoma.

In this study, we report three cases of CCS of the gastrointestinal tract showing distinctive pathologic and molecular characteristics compared with their soft tissue counterparts, including lack of melanocytic differentiation and the presence of a novel *EWS-CREB1* fusion transcript.

Materials and Methods

Case history patient 1. This 81-year-old woman underwent a hemicolectomy for a moderately differentiated adenocarcinoma of the transverse colon. The hemicolectomy specimen showed a synchronous CCS of the gastrointestinal tract in the ascending colon. Surgical

Authors' Affiliations: Departments of [1]Pathology and [2]Medicine, Memorial Sloan-Kettering Cancer Center, New York, New York, and [3]Department of Pathology, Brigham and Women's Hospital, Boston, Massachusetts

Received 12/27/05; revised 2/7/06; accepted 3/7/06.

The costs of publication of this article were defrayed in part by the payment of page charges. This article must therefore be hereby marked *advertisement* in accordance with 18 U.S.C. Section 1734 solely to indicate this fact.

Note: Supplementary data for this article are available at Clinical Cancer Research Online (http://clincancerres.aacrjournals.org/).

Requests for reprints: Marc Ladanyi, Department of Pathology, Memorial Sloan-Kettering Cancer Center, 1275 York Avenue, New York, NY 10021. Phone: 212-639-6369; Fax: 212-717-3515; E-mail: ladanyim@mskcc.org.

doi:10.1158/1078-0432.CCR-05-2811

margins were negative but there were regional lymph node metastases of CCS. The patient was then treated with 5-fluorouracil/leucovorin for 7 months for colon carcinoma. Intra-abdominal and liver metastases from the CCS were diagnosed after a 5-year interval and she underwent partial hepatectomy and removal of the peritoneal implants which provided the specimen submitted for molecular analysis. Electron microscopy was also done.

Case history patient 2. This 42-year-old woman underwent a segmental resection of the ileum for a primary CCS of the gastrointestinal tract. The surgery achieved negative margins and there was no lymph node involvement. This being a very recent case, no significant follow-up is available.

Case history patient 3. This 42-year-old woman underwent a liver biopsy in her work-up for the clinically presumed diagnosis of metastatic carcinoid tumor. A segmental resection of the ileum was done revealing a 3.7 circumferential partially obstructing lesion. In addition, a 5.0 cm mesenteric metastatic focus was identified. No further follow-up is available, this also being a recent case.

Immunohistochemistry and electron microscopy. Standard immunohistochemical studies were done. Prediluted antibodies were used for HMB45, A103, vimentin, CD34, Cam5.2, AE:AE3, NSE, CD56, synaptophysin, chromogranin, SMA, and HHF35 (all from Ventana Medical Systems, Tucson, AZ). For the other antibodies tested, we used the following conditions: CD117 (1:500; DAKO, Carpinteria, CA), desmin (1:50; DAKO), S100 protein (1:500; DAKO), MITF (1:200; DAKO), and tyrosinase (1:200; Novocastra, Newcastle upon Tyne, United Kingdom). Tissue for electron microscopy was available in case no. 1. Representative fresh tumor was fixed in 3% formaldehyde/3% glutaraldehyde, postfixed in 1% osmium tetroxide, embedded in epoxy resin, and stained with uranyl acetate-lead citrate by using standard procedures. Submitted electron microscopy prints were also available for review in case no. 3.

Fluorescence* in situ *hybridization analysis for the presence of EWS rearrangement. This was done in case nos. 1 and 2 using 50-μm paraffin sections. Whole nuclei preparations were obtained using standard protocols. The fluorescence *in situ* hybridization probes were the LSI *EWSR1* translocation probe pair (Abbott/Vysis, Downers Grove, IL), based on a break-apart fluorescence *in situ* hybridization assay design.

***Reverse transcription-PCR for* EWS-ATF1 *and* EWS-CREB1.** Frozen tissue, collected under an Institutional Review Board–approved protocol, was available in case no. 1. Total RNA was extracted using 1 mL of Trizol reagent (Life Technologies Inc., Gaithersburg, MD). In case nos. 2 and 3, RNA was extracted from a representative paraffin block of formalin-fixed tumor tissue, using the Paraffin Block RNA Isolation Kit (Ambion, Austin, TX). In all three samples, reverse transcription-PCR (RT-PCR) for the *EWS-ATF1* fusion was attempted first, using the forward primer EWSEx7-F1 and the reverse primer ATF1-R1 as reported previously (5). For RT-PCR detection of the *EWS-CREB1* transcript, we used the EWSEx7-F1 forward primer with either the CREB1ex7-REVC primer (specific for *CREB1*; sequence: GTACCC-CATCGGTACCATTGT) or the consensus CREB1ex7-REVA primer (binds both *CREB1* and *ATF1*; sequence: TCCATCAGTGGTCTGTG-CATACTG).

Long-range DNA PCR. DNA was extracted from fresh-frozen tissue using the Puregene DNA isolation Kit (Gentra Systems, Inc., Minneapolis, MN). PCR amplification of genomic DNA was done with HotStart master mix (Qiagen, Valencia, CA), first with EWSEx7-F1/CREB1-ex7REVB (5′-GTAGTACCCGGCTGAGTGGCTG-3′) and then with internal primers EWS-IVS7F (5′-GAGGCAGCTATTGCAGGC-3′) and CREB1-IVS6R (5′-CAACTGAAATATCCTATGGAACA-3′). The PCR amplification consisted of 15 minutes at 95°C, followed by 35 cycles of 30 seconds at 95°C, 30 seconds at 60°C, and 3 minutes at 72°C; a final extension of 10 minutes ended the reaction.

Sequencing. Direct sequencing of PCR products was done using the Big-Dye Terminator kit (Applied Biosystems, Foster City, CA) and run on an Applied Biosystems model 3100-Avant DNA sequencing system.

Hybridization of Affymetrix oligonucleotide chips. Adequate tumor tissue for RNA extraction was available in case no. 1 (CCS no. 1). RNA was isolated using RNAwiz RNA isolation reagent (Ambion) and run through a column with RNase-free DNase (Qiagen). Twenty-five nanograms of total RNA were tested for quality by RNA 6000 NanoAssay on a Bioanalyzer 2100 (Agilent, Palo Alto, CA). Two micrograms of high-quality total RNA ($A_{260/280}$ ratio > 1.8) was then labeled according to the manufacturer's instructions. Ten micrograms of labeled and fragmented cRNA were then hybridized onto a Human Genome U133A expression array (Affymetrix, Santa Clara, CA). Posthybridization staining, washing, and scanning were done according to instructions from the manufacturer (Affymetrix). The raw expression data were derived using the Affymetrix Microarray Analysis 5.0 (MAS 5.0) software. The data were normalized using a scaling target intensity of 500 to account for differences in the global chip intensity. The expression values were transformed using the logarithm base two. Affymetrix U133A gene expression data were also available in four cases of non-gastrointestinal CCS, all four carrying an *EWS-ATF1* fusion, as previously reported in a separate study (1).

Results

Morphology, immunohistochemical findings, and ultrastructure. Grossly, the lesions had a white-tan cut surface with infiltrative borders. Areas of hemorrhage and necrosis were also seen in some tumors. The mean tumor size was 5.7 cm and ranged from 3.7 to 7.5 cm. Microscopically, the tumors had a multinodular and infiltrative growth pattern, being centered in the submucosa and muscularis propria, but focally extending into the mucosa, as well as into subserosal fat. At low power, the tumors showed a variable growth pattern, with areas of solid, nested, single-file, and pseudo-papillary growth noted even within the same tumor (Fig. 1A and B). Morphologically, the tumors displayed predominantly uniform small epithelioid cells, with limited variation in the nuclear size and shape. However, ovoid cell morphology and even spindling was also noted. The nuclei showed a smooth nuclear contour, with open and fine chromatin, and prominent nucleoli. Although the main pattern included epithelioid cells with a minimal amount of cytoplasm arranged in solid nests, focal areas of more abundant cytoplasm, either clear or granular-eosinophilic, were noted in two cases (Fig. 1C). Particularly striking was the pseudo-papillary pattern with preservation of the tumor cells around blood vessels, mimicking an epithelial neoplasm with papillary architecture (Fig. 1B). No melanin pigment was identified. Scattered multinucleated, osteoclast-type giant cells were identified in one case (case no. 2, Fig. 1D). Mitotic activity was high in all three cases, with a mean of eight mitotic figures per 10 high-power fields.

The immunohistochemistry findings showed a consistent pattern, with diffuse and strong reactivity for S100 protein in the overwhelming majority of the tumor cells (Fig. 2A). All three cases showed staining for neural markers, such as NSE, CD56 and synaptophysin, either in a diffuse (case nos. 2 and 3) or focal (case no. 1) manner (Fig. 2B). Vimentin was only focally positive. The tumors were completely negative for all melanoma markers, such as HMB45, A103, MITF, and tyrosinase. All the other markers tested, including CD117, CD34, cytokeratins, muscle markers, and chromogranin were negative.

Ultrastructurally, the tumors examined (case nos. 1 and 3) showed moderate amounts of cytoplasm, rich in organelles

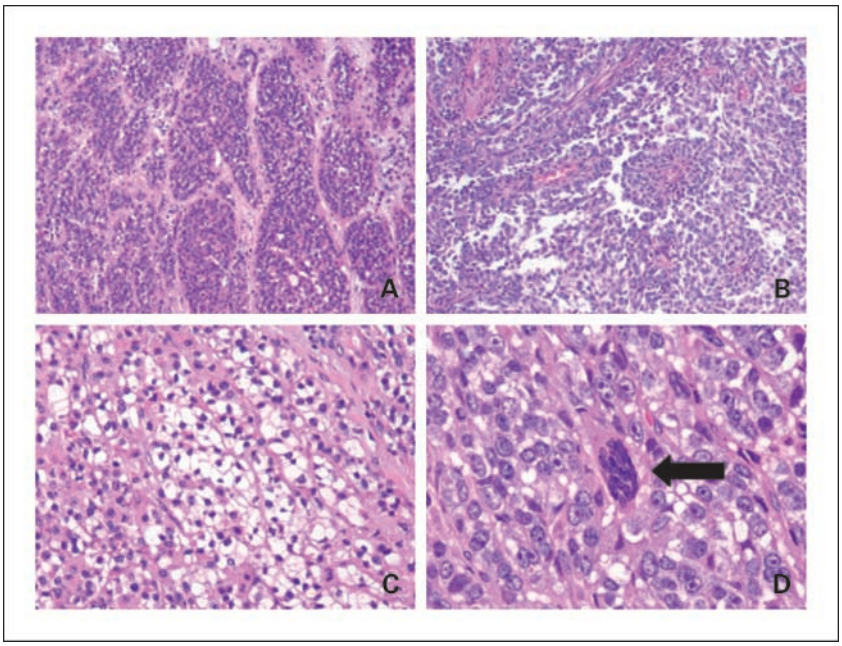

Fig. 1. Microscopic appearance of gastrointestinal CCS. *A,* well-defined nested growth pattern (case no. 2; magnification, ×100). *B,* focal pseudo-papillary pattern (case no. 1; magnification, ×100). *C,* areas of clear cell appearance (case no. 2; magnification, ×200). *D,* osteoclast-type giant cell (*arrow*; case no. 2; magnification, ×400).

such as mitochondria, polyribosomes, and lysosomes. A significant number of electron-dense granules of variable sizes and shapes were identified, but no diagnostic melanosomes or dense-core neurosecretory-type granules were identified (Fig. 2C). A number of primitive or simple cell junctions were seen. Pertinent negative findings included lack of basement membrane material, glycogen, myofilaments, and tonofilaments.

Detection of novel* EWS-CREB1 *fusion. Fluorescence *in situ* hybridization for *EWS* rearrangement was done in case nos. 1 and 2 and showed multiple nuclei with split signals indicative of *EWS* rearrangement in both (Fig. 3A). RT-PCR for the *EWS-ATF1* fusion was attempted in case no. 1, using the forward primer EWSEx7-F1 and the reverse primer ATF1-R1. This showed a weak but distinct product that differed in size from the product obtained from the *EWS-ATF1*-positive control cell line SU-CCS-1 (data not shown). Direct sequencing of the product in case no. 1 showed a chimeric transcript consisting of a junction between *EWS* exon 7 and a nucleotide sequence similar to *ATF1* exon 7, which BLAST analysis revealed to be a perfect match with exon 7 of *CREB1* (Fig. 3B). The novel *EWS-CREB1* fusion transcript was confirmed by RT-PCR using EWSEx7-F1 with a specific reverse primer CREB1-Ex7bR (Fig. 3C). Using the same respective primer pairs as above, case nos. 2 and 3 were negative by RT-PCR for the *EWS-ATF1* fusion, but were positive for *EWS-CREB1* showing the same fusion structure as case no. 1 (Fig. 3C and D). Thus, these three patients provide evidence for the existence of a recurrent variant chromosomal translocation of *EWS* (22q12) and *CREB1* (2q32.3), presumably a t(2;22)(q32.3;q12), in CCS. Alignment of the *EWS-CREB1* fusion product with native *ATF1* highlights the extensive similarity in *CREB1* and *ATF1* (Fig. 4).

Analysis of genomic structure of* EWS-CREB1 *fusion. Detailed genomic analyses of *EWS* breakpoints, available only for the *EWS-FLI1* fusions seen in Ewing's sarcomas, have shown that all fusions involving *EWS* exon 7 as the 5′ partner arise from genomic rearrangements within 4.2 kb downstream of *EWS*

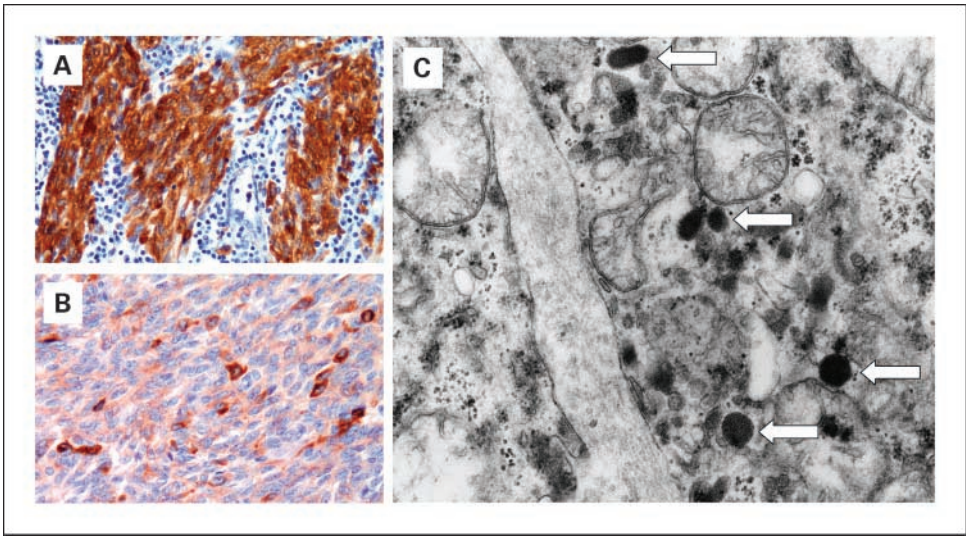

Fig. 2. Immunoprofile including (*A*) strong S100 protein reactivity (case no. 1, lymph node metastasis; magnification, ×200), and (*B*) focal synaptophysin staining (case no. 1; magnification, ×200). *C,* electron micrograph showing moderate amount of cytoplasm with a number of variably sized electron-dense granules (*arrows*). Diagnostic melanosomes or dense core neurosecretory granules were not identified (case no. 1, magnification, ×60,840).

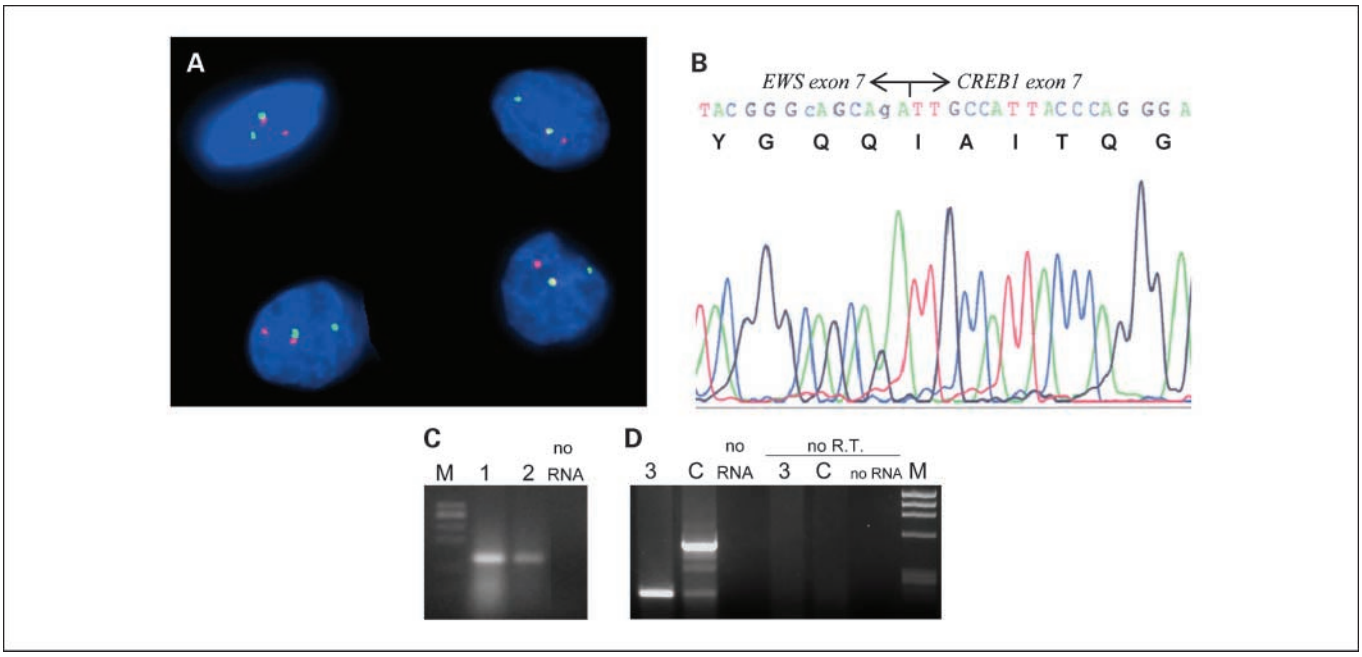

Fig. 3. *A,* fluorescence *in situ* hybridization for *EWS* rearrangement. The probe centromeric to *EWS* (*red*); the probe on the telomeric side of *EWS* (*green*). Four nuclei with split signals indicative of *EWS* rearrangement (case no. 1). *B,* electrophoretogram of direct sequencing of junction point of *EWS-CREB1* fusion transcript with in-frame fusion (case no. 1). *C* and *D*, agarose gels of *EWS-CREB1* RT-PCR products in case nos. 1 and 2 using primers EWSex7F1 and CREB1ex7REVc and in case no. 3 using the same forward primer but with reverse primer CREB1ex7REVa (consensus primer for *CREB1* and *ATF1*-see Fig. 4). Lane C is the SU-CCS-1 positive control cell line containing *EWS-ATF1*. No R.T. designates the negative controls lacking reverse transcriptase.

exon 7 (10). Likewise, it is likely that fusions involving *CREB1* exon 7 as the 3′ partner arise from genomic rearrangements of *CREB1* intron 6, which measures 4.95 kb. To characterize the genomic fusion point of the *EWS-CREB1* chimeric gene, we did PCR amplification of genomic DNA from case no. 1 with the EWSEx7-F1 and CREB1-ex7REVB primers. This revealed a strong discrete product of about 2 kb (data not shown). Stepwise direct sequencing of this fragment was done. PCR amplification and DNA sequencing with intronic forward primer EWS/IVS7F and the intronic reverse primer CREB1/IVS6R localized the genomic fusion point to nucleotide position g20493 of *EWS* intron 7 and nucleotide position g44998 of *CREB1* intron 6 (Supplementary Fig. S1A). The *EWS-CREB1* fusion gene in case no. 1 retained 1,052 bp from the 5′ end of *EWS* intron 7 and 913 bp from the 3′ end of *CREB1* intron 6 resulting in the formation a chimeric intron of 1,965 bp, which corresponded with the size of the initial long-range DNA PCR product.

In case nos. 2 and 3, only paraffin-embedded tissue was available for DNA extraction. PCR amplification of genomic DNA extracted from paraffin-embedded tissue was attempted in case no. 2 only. Long-range PCR using primers EWSEx7-F1 and

```
                    EWS exon 7                          CREB1 exon 7
EWS     AAATATAGCCAACAGAGCAGCAGCTACGGGCAGCAGAttgccattacccagggaggagca
                    ATF1 exon 4                 |||||||| |||      |||||
ATF1    CCAACTCCCATCTATCAGACTAGCAGCGGACAGTACAttgccattgccccaaatggagcc
                                                        ATF1 exon 5
                  ←CREB1ex7REVC primer
CREB1   atacagctggctaacaatggtaccgatggggtacagggcctgcaaacattaaccatgacc
         ||||| |||| |      || || ||||| |||||||| || || ||||||||||||||
ATF1    ttacagttggcaagtccaggcacagatggagtacagggacttcagacattaaccatgaca
                            ←ATF1-R1 primer
              ←CREB1ex7REVB primer          ←CREB1ex7REVA primer
CREB1   aatgcagcagccactcagccgggtactaccattctacagtatgcacagaccactgatgga
         ||| |||     |||||||  ||||| || ||||| |||||||||||||| ||||||||
ATF1    aattcaggcagtactcagcaaggtacaactattcttcagtatgcacagacctctgatgga

                                                        CREB1 exon 8
CREB1   cagcagatcttagtgcccagcaaccaagttgttgttcaagCTGCCTCTGGAGACGTACAA
         |||||||| | |||||||||||| || || || || ||| |||| || |||||  | |||
ATF1    cagcagatacttgtgcccagcaatcaggtggtcgtacaaaCTGCATCAGGAGATATGCAa
                                                        ATF1 exon 6
```

Fig. 4. Partial alignment of EWS-CREB1 fusion with native ATF1. Exons are indicated by alternating upper and lower case letters. The positions of reverse PCR primers in *CREB1* and *ATF1* are shown in italics. CREB1ex7REVC is a CREB1-specific primer, whereas CREB1ex7REVA is a consensus primer for *CREB1* and *ATF1*.

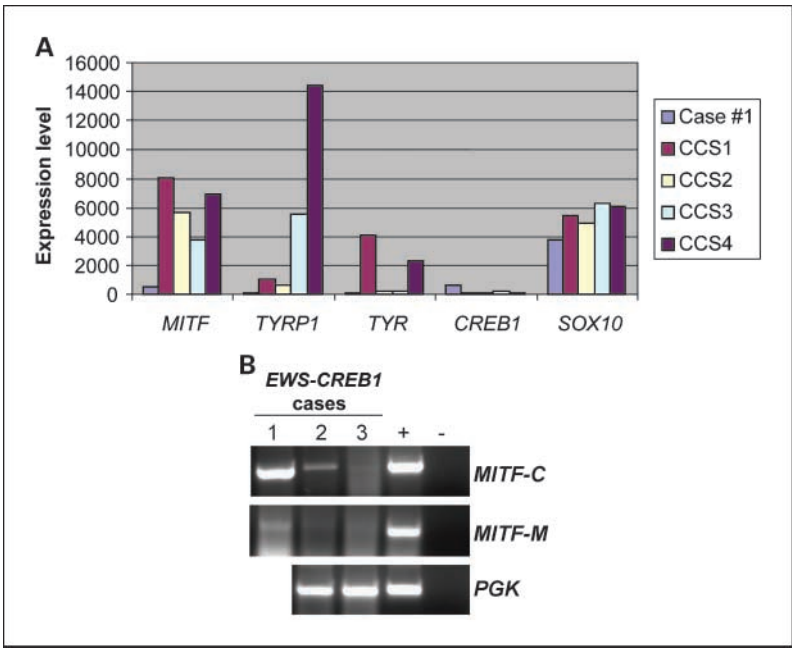

Fig. 5. Low or absent expression of melanocytic differentiation genes in CCS cases with the *EWS-CREB1* fusion. *A,* Affymetrix expression levels of melanocytic differentiation genes comparing *EWS-CREB1* case nos. 1 to 4 *EWS-ATF1*-positive CCS cases. The probe sets are 207233_s_at for *MITF* (microphthalmia-associated transcription factor), 205694_at for *TYRP1* (tyrosinase-related protein 1), 206630_at for tyrosinase (*TYR*), and 209842_at for *SOX10* (SRY-box 10). The data for *CREB1* (probe set 204314_s_at) are also shown. The values represent raw expression values calculated by Affymetrix MAS 5.0 software (no units). *B,* RT-PCR for consensus and melanocyte-specific *MITF* transcripts (*MITF-C* and *MITF-M*, respectively). In case nos. 2 and 3, which expressed little or no *MITF* transcripts, robust expression of a housekeeping gene (phosphoglycerate kinase, *PGK*) is shown, confirming RNA quality.

CREB1-ex7REVB primers did not yield a discrete PCR product. Prior to embarking on a more systematic set of long-range DNA PCR assays with regularly spaced primers in *EWS* intron 7 and *CREB1* intron 6, we wished to exclude the possibility of a similar genomic breakpoint in case no. 2 as in case no. 1. Therefore, we did a nested PCR using first the EWSEx7-F1 and CREB1-Ex7bR primers and then the internal primers EWS/IVS7F and CREB1/IVS6R. This amplified a strong 1 kb fragment (data not shown). Direct sequencing of this fragment revealed that the breakpoint was located at nucleotide position g20645 in *EWS* intron 7 and at nucleotide position g44921 of *CREB1* intron 6 (Supplementary Fig. S1B). Thus, the *EWS-CREB1* fusion gene in case no. 2 retained 1,204 bp from the 5′ end of *EWS* intron 7 and 992 bp from the 3′ end of *CREB1* intron 6, forming a chimeric intron of 2,196 bp.

RT-PCR and microarray analysis of melanocytic differentiation transcripts. Affymetrix U133A gene expression data were available in case no. 1 and were compared with data from four cases of non-gastrointestinal CCS, all four carrying the *EWS-ATF1* fusion, focusing on the level of expression of critical genes involved in melanogenesis. As shown in Fig. 5A, case no. 1 expressed lower levels of the key melanocytic genes *MITF*, *TYR*, and *TYRP1*, but *SOX10* transcript levels were not substantially different. This was consistent with its poor expression of melanocytic proteins by immunohistochemistry. We also examined the transcript levels of *CREB1* and *ATF1* (probe set 222103_at). The *CREB1* transcript level was higher in case no. 1 than in the four *EWS-ATF1* cases, possibly reflecting the detection of the *EWS-CREB1* transcript by this probe set. However, *ATF1* transcript levels did not differ between case nos. 1 and the 4 CCS with the *EWS-ATF1* fusion (data not shown).

There are several alternative forms of the *MITF* transcript, reflecting different promoters and transcription start sites, only one of which, *MITF-M*, is highly specific for the melanocytic lineage (5). We have previously shown that classic soft tissue CCS with *EWS-ATF1* express the melanocyte-specific *MITF-M* transcript, further supporting their genuine melanocytic differentiation (5). In contrast, RT-PCR analysis for the *MITF-M* transcript in our three EWS-CREB1 cases was negative in two cases and only weakly positive in one case (Fig. 5B), the latter being case no. 1, which also expressed the highest level of the consensus *MITF* transcript among these three cases (Fig. 5B). Together with the above immunohistochemical and ultrastructural studies, these gene expression data confirm that evidence of melanocytic differentiation in CCS with *EWS-CREB1* is either absent or much less than in classic CCS with *EWS-ATF1*. This, in turn, strengthens the notion that melanocytic features are not a necessary finding in this type of sarcoma.

Discussion

The classic cytogenetic hallmark of CCS, first described in cases arising in somatic soft tissues, is a recurrent t(12;22)(q13;q12) translocation, resulting in the *EWS-ATF1* fusion (3, 5, 6), an alteration which was, until recently (see below), not observed in any other tumor type. Despite this distinctive gene fusion in CCS (absent in melanoma; refs. 4, 11) and the absence of the *BRAF* mutations that are so common in melanoma (2), immunohistochemistry and ultrastructural studies of CCS suggest that it is, like melanoma, a neuroectodermal tumor with melanocytic differentiation. Further evidence of the genuine melanocytic differentiation in CCS has been provided by a microarray-based gene expression profiling study which showed that unsupervised clustering grouped CCS with melanomas rather than with other high-grade sarcomas (1). This study also confirmed the up-regulation in CCS of a number of genes involved in melanocytic differentiation (such as *MITF* and *SOX10*), relative to other soft tissue sarcoma types.

We have identified a novel recurrent variant fusion in CCS, *EWS-CREB1*. *CREB1* maps to 2q34, and like *EWS*, is oriented with its 3′ end telomeric, suggesting that both of our cases may have contained a simple t(2:22)(q34;q12) at the cytogenetic

level, but no karyotypes were available. Our finding that all three CCS cases with this novel fusion arose in the gastrointestinal tract suggests that this fusion may be preferentially associated with a gastrointestinal location, whereas non-gastrointestinal CCS show the *EWS-ATF1* fusion in at least 90% of the cases (5, 6).

ATF1, cyclic AMP (cAMP)–responsive element binding protein (CREB1), and cAMP response element modulatory protein constitute a subfamily of the basic leucine zipper superfamily of transcription factors and have been implicated in cAMP and Ca^{2+}-induced transcriptional activation. CREB1 is a nuclear protein that binds cAMP response elements as a homodimer or heterodimer (with members of the ATF and AP1 transcription factor families). Overexpression of CREB transcription factors contributes to the acquisition of the metastatic potential in human melanoma cells and is also oncogenic in the myeloid lineage (12, 13). Genome-wide screens for promoters bound by CREB reveal a very large number of potential target genes (~4,000) and a critical role for tissue-specific coactivators in determining target gene activation (14).

Like other members of the basic leucine zipper superfamily, CREB1 has a modular structure consisting of a carboxyl terminal basic leucine zipper domain mediating DNA binding and dimerization, and an amino terminal transactivation domain that contains a kinase-inducible domain mediating interactions with CBP and p300 (Fig. 6). The predicted protein structure of EWS-CREB1 thus parallels that of EWS-ATF1 (Fig. 6). Specifically, all CCS cases with *EWS-ATF1* contain fusion transcripts in which the basic leucine zipper domain is retained, and this is also the case for *EWS-CREB1*. The kinase-inducible domain, which is either excluded or truncated in different forms of EWS-ATF1, is not part of EWS-CREB1 in the three current cases (Fig. 6). Thus, the structure of EWS-ATF1 and the predicted structure of EWS-CREB1 indicates that mediating cAMP-inducible transcription through PKA-mediated phosphorylation is not a necessary feature of either fusion protein. Interestingly, whereas the *MITF-M* promoter is cAMP-inducible in the presence of SOX10 in melanoma cells through binding of its cAMP response elements by CREB (15), EWS-ATF1 does not seem to transactivate the *MITF-M* promoter in CCS cells, at least in exogenous constructs (16). Thus, the expression of the *MITF-M* transcript in CCS may represent a feature of the precursor cell in which the translocation occurs. Indeed, a chromatin immunoprecipitation–based screen for EWS-ATF1 target genes in a CCS cell line did not detect MITF (17). In fact, none of the nine putative target genes isolated in that study were related to the melanocytic lineage. Another line of evidence that EWS-ATF1 and *MITF-M* expression are not tightly linked comes from data in angiomatoid fibrous histiocytoma. Some angiomatoid fibrous histiocytomas seem to contain a novel *FUS-ATF1* fusion (18, 19) but there is a recent report of a case with an *EWS-ATF1* fusion, and that case lacked expression of the melanocytic splice form of MITF (20).

The occurrence of CCS in the gastrointestinal tract is exceptionally rare. Data from eight genetically confirmed cases along with the three current *EWS-CREB1* cases and two additional unpublished cases from our center are summarized in Supplementary Table S1 (7–9, 21–23). Based on these 13 cases, CCS of the gastrointestinal tract seems slightly more prevalent in females, with a wide age distribution, 15 to 85 years, but with eight cases (62%) occurring between 30 and 51. The most common location is the small bowel (69%) followed by colon and stomach. A common characteristic of these tumors is the transmural involvement of the bowel wall, often with mucosal ulceration and spreading to regional lymph nodes. Microscopically, the predominant pattern is of nested or solid growth of small epithelioid cells with amphophilic or clear cytoplasm and uniform nuclei with conspicuous nucleoli. However, certain cases contain somewhat distinctive morphologic features, due to a component of admixed reactive, KP1-positive, and osteoclast-type giant cells (9, 23). One of our cases showed a similar, although very minor, component of osteoclast-type giant cells. These cells are most likely reactive histiocytic cells, and are different morphologically and immunohistochemically from the multinucleated tumor cells seen in conventional CCS. This latter type of giant tumor cell was not seen in most cases of primary gastrointestinal CCS. Due to its unusual visceral presentation, coupled with the inconsistent expression of melanocytic markers and variant *EWS* fusion partners, CCS of the gastrointestinal tract can often be misdiagnosed. This is evident in our experience, in which the original or second-opinion consultation diagnoses included: poorly differentiated carcinoma, most likely metastatic from the other synchronous colonic primary adenocarcinoma (case no. 1); carcinoid tumor, gastrointestinal stromal tumor, and undifferentiated neoplasm, possibly neurogenic in origin (case no. 2); and metastatic melanoma and carcinoid tumor (case no. 3).

Interestingly, whereas non-gastrointestinal CCS shows the expression of melanocytic markers (HMB45, A103, MITF, etc.) in the overwhelming majority of cases (5), the reverse seems to be the case in the gastrointestinal tract, where most tumors (69%) are negative for these markers (Supplementary Table S1). In spite of the negativity for melanocytic markers, the morphologic appearance coupled with the t(12;22) translocation supports a diagnosis of CCS in such cases. Although all three of our *EWS-CREB1*-positive CCS lacked melanocytic expression by immunohistochemistry, this was also noted in

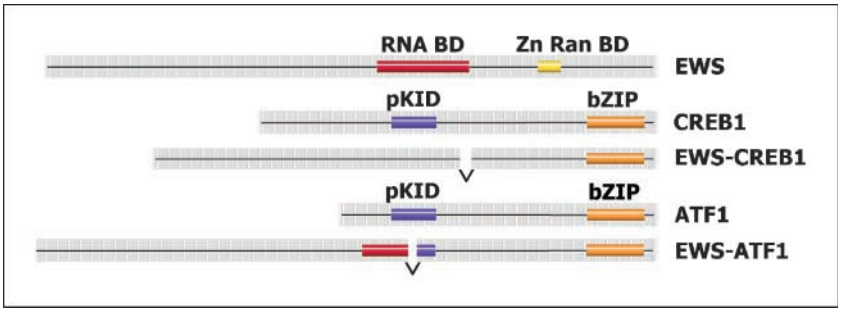

Fig. 6. Schematic scale diagram of normal EWS, CREB1, and ATF1 proteins and corresponding fusion products. Zn Ran BD, zinc finger RAN binding domain in EWS; pKID, kinase-inducible domain, part of the transactivation domain of CREB family transcription factors; bZIP, basic-leucine zipper domain, representing the DNA-binding domain. Scale is 10 amino acid residues/segment. In the predicted EWS-CREB1 fusion protein, codon 265 of EWS is joined to codon 182 of CREB1. The diagram shows only the most common type of EWS-ATF1 fusion protein, in which EWS codon 325 is joined to ATF1 codon 65. Data for native proteins is from InterPro database at http://www.ebi.ac.uk/interpro.

four of eight previously reported *EWS-ATF1*-positive CCS of the gastrointestinal tract (9, 21, 23, 24), suggesting that gastrointestinal location rather than the fusion transcript type might determine the lack of melanocytic differentiation. Furthermore, two additional gastrointestinal CCS from our files (not previously reported, see Supplementary Table S1), showing either *EWS-ATF1* by RT-PCR or *EWS* rearrangement by FISH lacked evidence of melanocytic differentiation by immunohistochemistry. The consistent expression of neuroectodermal markers, such as S100, NSE, CD56, and synaptophysin, in our cases, raises the possibility of a novel gastrointestinal neuroectodermal tumor carrying an *EWS-CREB1* fusion and lacking melanocytic differentiation. However, the detection of *EWS-ATF1* fusion in a number of gastrointestinal tract CCS also lacking expression of melanocytic markers, argue in favor of a common histogenesis, possibly from a gastrointestinal neuroectodermal precursor cell which has lost or does not have potential to differentiate along the melanocytic lineage, in contrast to the putative neuroectodermal precursor cell of non-gastrointestinal CCS.

Finally, we note that the clinical behavior of gastrointestinal CCS seems to be aggressive, regardless of the fusion type, with a high incidence of both distant and regional metastases. Most patients developed liver metastases, but intraperitoneal spread was noted in a few cases as well. The time to distant recurrence was variable, ranging from 9 months to 5 years.

Acknowledgments

The authors thank Tao Zheng for expert technical assistance with RT-PCR and Dr. Agnes Viale and the staff of the Memorial Sloan-Kettering Cancer Center Genomics Core Laboratory for assistance with microarray studies.

References

1. Segal NH, Pavlidis P, Noble WS, et al. Classification of clear-cell sarcoma as a subtype of melanoma by genomic profiling. J Clin Oncol 2003;21:1775–81.
2. Panagopoulos I, Mertens F, Isaksson M, Mandahl N. Absence of mutations of the BRAF gene in malignant melanoma of soft parts (clear cell sarcoma of tendons and aponeuroses). Cancer Genet Cytogenet 2005;156:74–6.
3. Zucman J, Delattre O, Desmaze C, et al. EWS and ATF-1 gene fusion induced by t(12;22) translocation in malignant melanoma of soft parts. Nature Gene 1993;4:341–5.
4. Langezaal SM, Graadt van Roggen JF, Cleton-Jansen AM, Baelde JJ, Hogendoorn PC. Malignant melanoma is genetically distinct from clear cell sarcoma of tendons and aponeurosis (malignant melanoma of soft parts). Br J Cancer 2001;84:535–8.
5. Antonescu CR, Tschernyavsky SJ, Woodruff JM, et al. Molecular diagnosis of clear cell sarcoma: detection of EWS-ATF1 and MITF-M transcripts and histopathological and ultrastructural analysis of 12 cases. J Mol Diagn 2002;4:44–52.
6. Panagopoulos I, Mertens F, Debiec-Rychter M, et al. Molecular genetic characterization of the EWS/ATF1 fusion gene in clear cell sarcoma of tendons and aponeuroses. Int J Cancer 2002;99:560–7.
7. Covinsky M, Gong S, Rajaram V, Perry A, Pfeifer J. EWS-ATF1 fusion transcripts in gastrointestinal tumors previously diagnosed as malignant melanoma. Hum Pathol 2005;36:74–81.
8. Taminelli L, Zaman K, Gengler C, et al. Primary clear cell sarcoma of the ileum: an uncommon and misleading site. Virchows Arch 2005;447:772–7.
9. Zambrano E, Reyes-Mugica M, Franchi A, Rosai J. An osteoclast-rich tumor of the gastrointestinal tract with features resembling clear cell sarcoma of soft parts: reports of 6 cases of a GIST simulator. Int J Surg Pathol 2003;11:75–81.
10. Zucman-Rossi J, Legoix P, Victor JM, Lopez B, Thomas G. Chromosome translocation based on illegitimate recombination in human tumors. Proc Natl Acad Sci U S A 1998;95:11786–91.
11. Patel RM, Downs-Kelly E, Weiss SW, et al. Dual-color, break-apart fluorescence *in situ* hybridization for EWS gene rearrangement distinguishes clear cell sarcoma of soft tissue from malignant melanoma. Mod Pathol 2005;18:1585–90.
12. Jean D, Bar-Eli M. Regulation of tumor growth and metastasis of human melanoma by the CREB transcription factor family. Mol Cell Biochem 2000;212:19–28.
13. Shankar DB, Cheng JC, Kinjo K, et al. The role of CREB as a proto-oncogene in hematopoiesis and in acute myeloid leukemia. Cancer Cell 2005;7:351–62.
14. Zhang X, Odom DT, Koo SH, et al. Genome-wide analysis of cAMP-response element binding protein occupancy, phosphorylation, and target gene activation in human tissues. Proc Natl Acad Sci U S A 2005;102:4459–64.
15. Huber WE, Price ER, Widlund HR, et al. A tissue-restricted cAMP transcriptional response: SOX10 modulates α-melanocyte-stimulating hormone-triggered expression of microphthalmia-associated transcription factor in melanocytes. J Biol Chem 2003;278:45224–30.
16. Li KK, Goodall J, Goding CR, et al. The melanocyte inducing factor MITF is stably expressed in cell lines from human clear cell sarcoma. Br J Cancer 2003;89:1072–8.
17. Jishage M, Fujino T, Yamazaki Y, Kuroda H, Nakamura T. Identification of target genes for EWS/ATF-1 chimeric transcription factor. Oncogene 2003;22:41–9.
18. Waters BL, Panagopoulos I, Allen EF. Genetic characterization of angiomatoid fibrous histiocytoma identifies fusion of the FUS and ATF-1 genes induced by a chromosomal translocation involving bands 12q13 and 16p11 [In Process Citation]. Cancer Genet Cytogenet 2000;121:109–16.
19. Raddaoui E, Donner LR, Panagopoulos I. Fusion of the FUS and ATF1 genes in a large, deep-seated angiomatoid fibrous histiocytoma. Diagn Mol Pathol 2002;11:157–62.
20. Hallor KH, Mertens F, Jin Y, et al. Fusion of the EWSR1 and ATF1 genes without expression of the MITF-M transcript in angiomatoid fibrous histiocytoma. Genes Chromosomes Cancer 2005;44:97–102.
21. Donner LR, Trompler RA, Dobin S. Clear cell sarcoma of the ileum: the crucial role of cytogenetics for the diagnosis. Am J Surg Pathol 1998;22:121–4.
22. Fukuda T, Kakihara T, Baba K, et al. Clear cell sarcoma arising in the transverse colon. Pathol Int 2000;50:412–6.
23. Friedrichs N, Testi MA, Moiraghi L, et al. Clear cell sarcoma-like tumor with osteoclast-like giant cells in the small bowel: further evidence for a new tumor entity. Int J Surg Pathol 2005;13:313–8.
24. Pauwels P, Debiec-Rychter M, Sciot R, et al. Clear cell sarcoma of the stomach. Histopathology 2002;41:526–30.